European Journal of Soil Science, June 1997, **48**, 227–237

A hard sandy-loam soil from semi-arid Northern Cameroon: II. Geochemistry and mineralogy of the bonding agent

M. LAMOTTE[a], A. BRUAND[b], D. OHNENSTETTER[c], P. ILDEFONSE[d] & G. PÉDRO[e]

[a]*ORSTOM, Département TOA, UR 12, 213 rue La Fayette, 75480 Paris;* [b]*INRA, Unité de Science du sol–SESCPF, Centre de Recherche d'Orléans, Avenue de la Pomme de Pin, 45160 Ardon;* [c]*CNRS, CRPG, 15 rue Notre-dame-des-Pauvres, 54501 Vandœuvre-les-Nancy;* [d]*Université Paris 7, Laboratoire de Minéralogie–Cristallographie, UA CNRS 09, 4 place Jussieu, 75252 Paris Cedex 05, and* [e]*INRA, Unité de Science du Sol, Route de Saint-Cyr, 78026 Versailles Cedex, France*

Summary

The hardening of soils containing little clay content has often been related to the cementing of skeleton grains. In sandy-loam soils from the southern plain of the Chad basin the skeleton grains of the hard horizon are coated and bonded by wall-shaped bridges. We have studied the bonding agent by X-ray diffraction on extracted fractions (<0.5 μm) and by quantitative *in situ* electron microprobe analysis on thin sections. The coatings and the wall-shaped bridges are composed mainly of SiO_2 (mean = 60%), Al_2O_3 (29%) and Fe_2O_3 (7%). The TiO_2 and K_2O contents were small (1–2%), and the MgO, Na_2O and CaO contents were less than 1%. The composition of the coatings and the wall-shaped bridges is almost homogeneous, even if the Si/Al atomic ratio varies weakly with the morphology of the bridges. The bonding agent constituting the coatings and the wall-shaped bridges seems to be a mixture of predominantly Al-Fe beidellite with small contents of kaolinite, illite and quartz. A small content of fine clay minerals plays the major role of bonding agent and is responsible for hardness in sandy or sandy-loam soils.

Un sol sablo-limoneux à forte cohésion du Nord-Cameroun: II. Géochimie et minéralogie du liant

Résumé

Le durcissement des sols peu argileux a souvent été expliqué par le développement de ciments entre les grains du squelette. Au sein d'un sol sablo-limoneux de la plaine méridionale du bassin tchadien, l'horizon à forte cohésion qui est généralement présent à la base d'un horizon meuble se distingue par le mode d'assemblage des constituants élémentaires: les grains du squelette sont revêtus et reliés entre eux par des cloisons. Nous avons déterminé la composition géochimique des revêtements et des cloisons, puis nous l'avons interprétée en terme minéralogique. Cette étude a été réalisée par diffraction des rayons X sur une fraction extraite (<0.5 μm) et par microanalyse quantitative *in situ* sur des lames-minces. Les revêtements et les cloisons sont constitués principalement de SiO_2 (moyenne = 60%), Al_2O_3 (29%) et Fe_2O_3 (7%), les autres composés étant TiO_2 et K_2O (1-2%), MgO, Na_2O et CaO ($\leqslant$1%). Le rapport atomique Si/Al varie faiblement avec la morphologie des cloisons mais, dans l'ensemble, la composition des revêtements et des cloisons est homogène. Le liant qui les constitue semble être un mélange composé principalement de beidellite alumino-ferrifère, et secondairement de kaolinite, d'illite et de quartz en proportion faible. Les minéraux argileux de petite taille et en faible quantité jouent le rôle de liant et sont responsables de la forte cohésion dans des sols sableux ou sablo-limoneux.

Correspondence: A. Bruand. E-mail: ary.bruand@orleans.inra.fr
Received 27 June 1996; revised version accepted 13 December 1996

Introduction

Many soils have strong horizons, such as duripans (Soil Survey Staff, 1975), fragipans (e.g. Soil Survey Staff, 1975; Smeck & Ciolkosz, 1989) or hardsetting horizons (e.g. McDonald *et al.*, 1984; Mullins & Ley, 1995). The two latter types of horizon are hard when dry but slake in water. The presence of a cement, particularly composed of silica, is clearly associated with duripan (e.g. Chartres & Fitzgerald, 1990; Milnes *et al.*, 1991; Balbir-Singh & Gilkes, 1993). The nature of the agent which bonds the skeleton grains in fragipan and hardsetting horizons, and thus induces their strength in the dry state is still unclear.

In most previous studies, the bonding agent has been analysed on the fine fraction extracted from the soil. Lozet & Herbillon (1971) studied a fragipan and showed no particular chemical cementing agent. Several studies of fragipan concluded that the cementing agent was probably composed of sesquioxide (Grossman *et al.*, 1959), clay (Jha & Cline, 1963), or silica, possibly mixed with aluminosilicate (Harlan *et al.*, 1977; Franzmeier *et al.*, 1989). Microscopic observations of fragipan showed that the sand or silt grains were coated and bonded together by bridges (Yassoglou & Whiteside, 1960). These authors suggested that the 2 : 1 clay minerals identified by X-ray diffraction on the extracted fraction composed both the coatings and the bridges. Thus, they considered that the 2 : 1 clay minerals were responsible for the fragipan strength but they also involved the role of colloidal silica or soluble aluminium. Wang *et al.* (1974) and Lindbo & Veneman (1989) supported the clay bridge hypothesis to explain the behaviour of fragipan. For all of these studies, the fine material extracted probably incorporated components that have no role in the hardening.

In other studies the bonding agent was analysed *in situ* to avoid taking into account components not involved in hardening. In a fragipan from South Wales, Bridges & Bull (1983) observed intergranular bridges with SEM and then analysed their composition by *in situ* qualitative microanalysis. They found a large content of silica and little of Al, K and Fe. They concluded that amorphous silica bridges were responsible for the strength of the fragipan. Their results could also be interpreted as corresponding to clay bridges with locally underlying quartz which overestimated the Si content of the studied bridges. Norton *et al.* (1984) studied the bonding agent of the fragipan in soils of east-central Ohio on etched thin sections by combining optical transmission microscopy, electron scanning microscopy and electron probe microanalysis to avoid the presence of underlying grains. The qualitative EDXRA results obtained for the intergranular bridging material showed a high Si peak with smaller Al, K and Fe peaks. The authors concluded that the large Si content was the main characteristic of the bridges which incorporated Si-rich hydrous aluminosilicate and clay minerals. Chartres & Fitzgerald (1990) examined the bonding agent in hardsetting horizons from Australian soils using SEM–EDXRA and TEM–EDXRA. The submicroscopic observations and the semiquantitative analyses (estimation of Si/Al ratio) suggested that there was a mixture of clay minerals and amorphous silica in the intergranular bridges. They concluded that amorphous silica and precipitated aluminosilicates play some role in hardsetting. On the contrary, amorphous silica was clearly the main agent of irreversible cementation in both duripan and saprolite samples, which were also examined. Thus, at present, only qualitative or semiquantitative results have been obtained by *in situ* chemical microanalysis of the bonding agent in the soils which are hard in their dry state but which slake in water.

We have studied by quantitative *in situ* electron microprobe analyses the geochemistry and the mineralogy of the bonding agent of the intergranular wall-shaped bridges responsible for the hardness of a sandy-loam horizon in northern Cameroon (Part I) (Lamotte *et al.*, 1997).

Soil and sampling

We studied a solodic Planosol (FAO–UNESCO, 1975), in northern Cameroon. It has an abrupt transition at 35 cm depth between a loose and a hard horizon. Lamotte *et al.* (1997) give details about the site (*hardé Lagadgé*) and the soil. The hard horizon is characterized by a specific fabric: the skeleton grains are coated and linked together by wall-shaped bridges. Both coatings and bridges are composed mainly of very small particles (<0.2 μm) including some fine grains 1–3 μm in size. The coatings and wall-shaped bridges exhibited a large range in morphology and in size. In the loose horizon the skeleton grains are generally uncoated and free from linkages. Lamotte (1995) showed that the skeleton grains consist of quartz ($\geqslant 95\%$), weathered K-feldspars ($\leqslant 4\%$) and heavy minerals ($<1\%$), and that pedofeatures (Fe oxide nodules, clay coatings within vughs and fine silty-clay capping on coarse skeleton particles) are scarce.

We collected disturbed samples for mineralogical study in the loose horizon at 22 cm depth and in the hard horizon at 40 cm, 57 cm, 67 cm and 102 cm from the soil surface. Both undisturbed and orientated soil samples were also collected from the hard horizon, at 45 cm depth, for thin section preparation.

Laboratory methods

X-ray diffraction analysis

Disturbed samples were dispersed in distilled water by mechanical shaking for 16 h. Then, the <0.5 μm fraction was separated from the suspension by sedimentation (pipette sampling and centrifuging). For each sampled fraction, two preparations were made: randomly orientated powder (P) and orientated deposit which was studied in three conditions, at 25°C (L), after treatment with glycerol (G) and after heating at 500°C (D). The samples were scanned from 3 to 70°2θ for P

powders and from 3 to 15°2θ for the L, G and D deposits using a Siemens D 500 diffractometer with the Cu-Kα radiation.

Microscopic observation

The thin sections (30 × 45 mm) were prepared as described by Lamotte *et al.* (1997). Then the polished surfaces were coated with carbon deposit for optical and scanning electron microscopy (SEM). The latter were made to select and describe sites of coatings and wall-shaped bridges prior to their study by electron probe microanalysis (EPMA). Optical microscopic examination at magnification of ×80–300 was carried out using a Zeiss Universal polarizing microscope fitted with both transmitted and incident light facilities. Scanning electron microscopy at magnification of ×300–1500 was carried out on a Cambridge 90B instrument using the backscattered electrons mode (Lloyd, 1987).

Only two types of site were selected for the chemical analysis (Fig. 1a, b). The bridges in small intergranular voids, <5 μm in size (Fig. 1c), were not studied because the skeleton grains were so close, that we could not analyse the bridges alone. The sites with bridges and coatings with underlying or included skeleton grains (Fig. 1d, e) were also eliminated after examination by optical microscopy under cross-polarized light at high magnification because we could not avoid the inclusion of skeletal grains in the chemical determinations. The six selected sites (referred to as I to VI) for *in situ* microanalysis were described and photographed using SEM to obtain detailed pictures prior to chemical microanalysis.

Microanalysis

Chemical composition for Si, Al, Fe, Ti, Mn, K, Mg, Ca, Na, P and S was determined using a Camebax Datanim electron microprobe equipped with four wavelength-dispersive spectrometers (WDS) and combined with the ZAF–MBXCOR quantitative analysis software (Pouchou, 1987). An accelerating voltage of 15 kV, a probe current of 4 nA and a 15 s count time were used. The beam was 1 μm in diameter (3–5 μm^3 in volume). Measurements on standard minerals were recorded to transform WDS signal to elemental content. Total iron was expressed as Fe_2O_3, and all the results are presented and discussed on a basis that the sum of oxides' mass equals 100.

Several chemical determinations were made in the middle of large intergranular voids to study the interaction of the electrons beam with the impregnated polyester resin or with the underlying glass slide. The sum of oxides was always about 0.1%. Thus, the polyester resin and the underlying glass slide did not affect the chemical determinations. Because of possible instrument deviation, a calibration test was made on a reference K-feldspar grain in the thin section after every 20 measurements.

Results

Mineralogy of the <0.5 μm extracted fractions

The <0.5 μm fraction of the loose horizon (Fig. 2a) comprised poorly ordered kaolinite (0.721, 0.358 and 0.238 nm), quartz (0.426, 0.335 and 0.246 nm) and 2 : 1 clay minerals. For the latter, the XRD indicated the presence of variable d-spacing (wide maximum between 1 and 1.6 nm on the L diffractogram and weak maximum at 1.017 nm on the G diffractogram).

In the samples of the hard horizon, the XRD showed kaolinite, quartz and 2 : 1 clay minerals (Fig. 2b, c). The peaks at 1.017 nm on the G diffractogram indicated the presence of nonexpanding 2 : 1 clay (illite). The other 2 : 1 clay minerals, with variable d-spacing (smectite) were identified with their

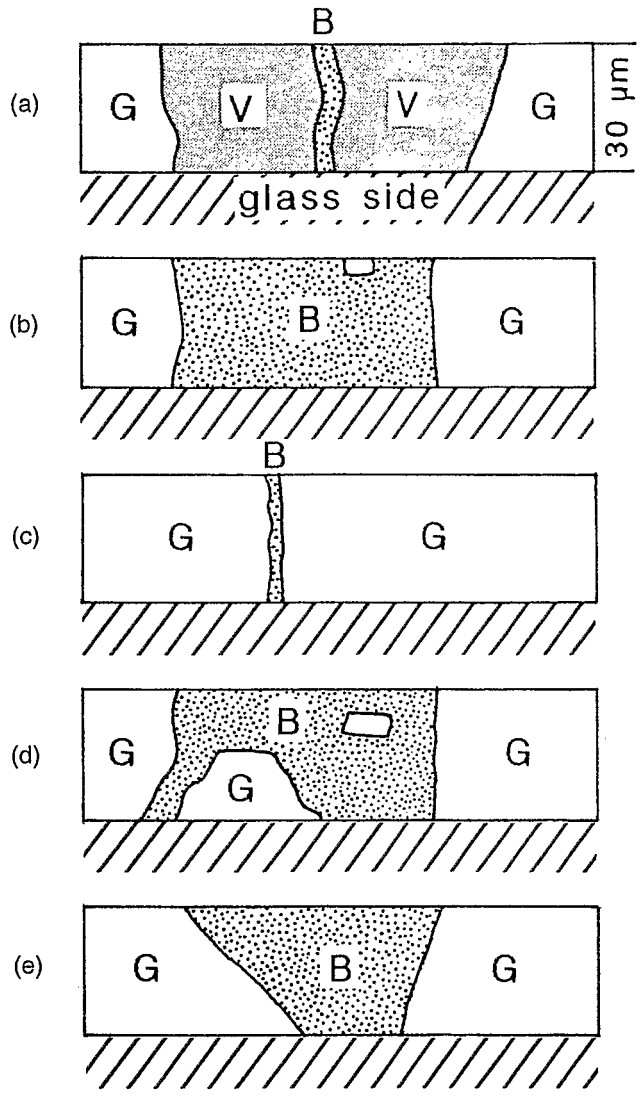

Fig. 1 Sketch showing the different types of site for which the chemical composition of the wall-shaped bridges could be analysed (B, bridge; V, void; G, skeleton grain).

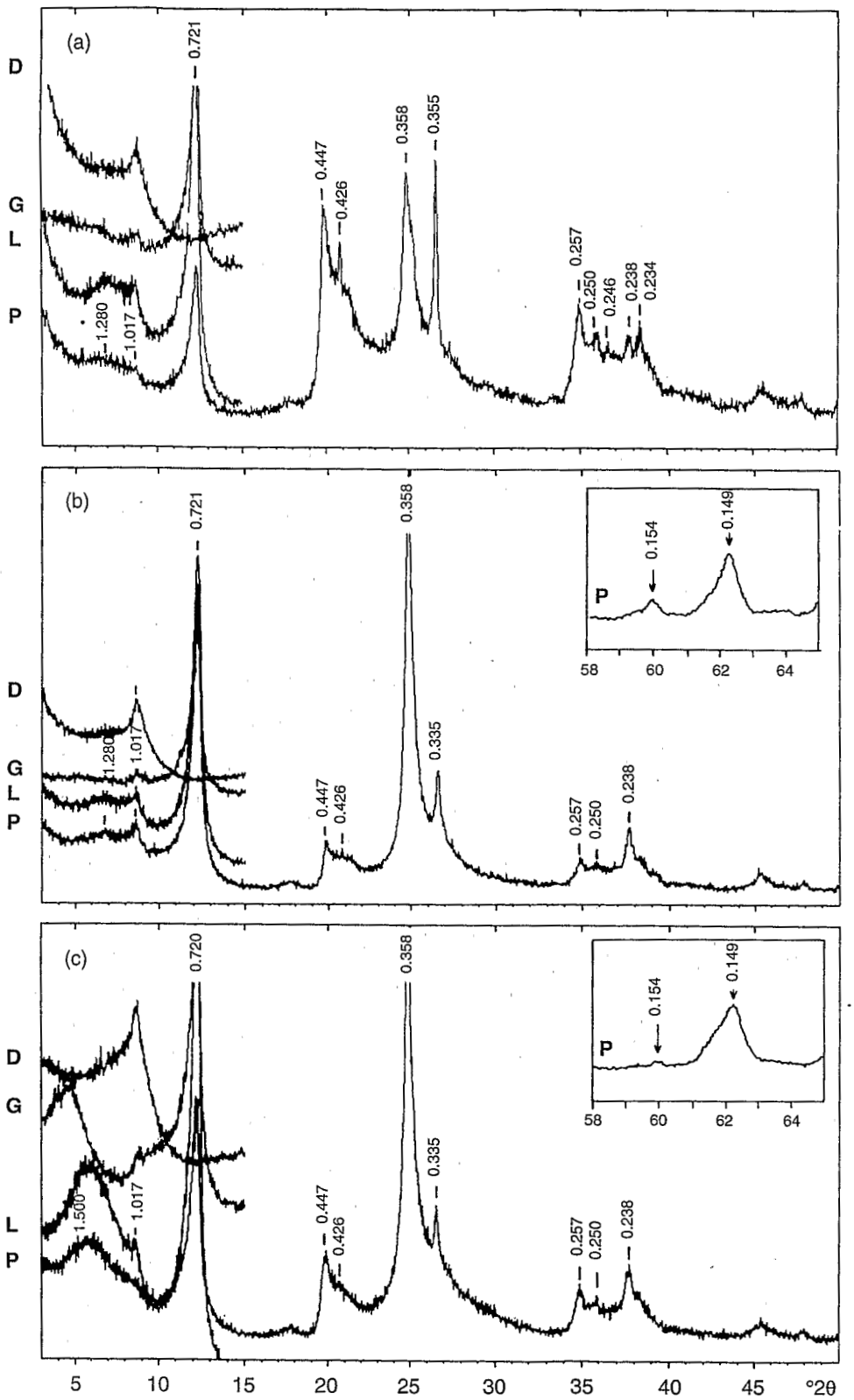

Fig. 2 X-ray diffraction (Cu-Kα) patterns obtained from the extracted <0.5 μm clay fractions: (a) for the loose horizon at 22 cm depth, (b) and (c) for the hard horizon at 40 and 102 cm depth, respectively (P, randomly-orientated powder; L, deposit under laboratory conditions; G, deposit with vaporised glycerol; and D, 500°C dried deposit).

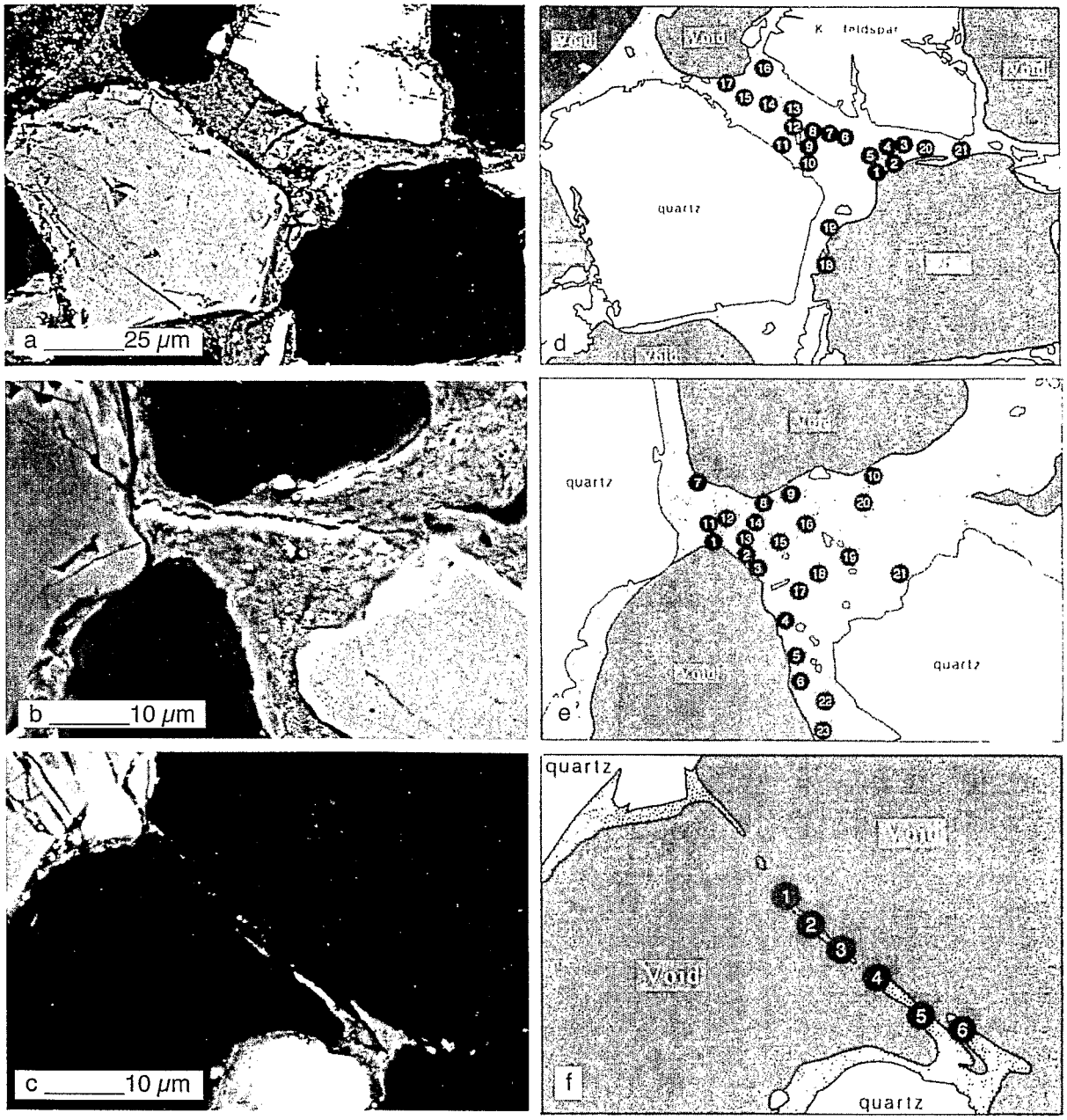

Fig. 3 Backscattered electron images (a) of site I (×900), (b) site II (×1500), and (c) site III (× 1600) selected for electron probe microanalysis (EPMA) of wall-shaped bridges and coatings (black areas are voids, homogeneous grey areas are skeleton grains, heterogeneous dark greyish areas are clay particles with associated interparticle voids). Outline sketches of sites I (d), II (e) and III (f) showing the location of the EPMA points with their marked reference numbers.

peaks at 1.3–1.5 nm on the P and L diffractograms, and at 1.9 nm on the G diffractograms. They did not appear on the D diffractograms (Fig. 2b, c). The intensities of the 1.3–1.5 nm maximum increased significantly at 102 cm depth.

Microprobe analysis of wall-shaped bridges and coatings

Site I showed a short and thick wall-shaped bridge (45 μm thick) between two coated skeleton grains (quartz and weathered K-feldspar) about 15 μm away from one another (Fig. 3a, d). The bridge included several angular and fine quartz grains (0.5–3 μm in size). Chemical analysis of the fine material constituting both the bridge and the coatings of the skeleton grains showed that SiO_2 (52–57%), Al_2O_3 (29–35%) and Fe_2O_3 (7–11%) were the major components (Table 1). The Si/Al atomic ratio ranged from 1.3 to 1.6 (mean = 1.44, standard deviation = 0.08). The associated components were K_2O and TiO_2 (1–3%). The contents of MgO, Na_2O and CaO

Table 1 Chemical composition (EPMA data) for the site I (Fig. 3a and d). The analysed points were located in the wall-shaped bridge (points No. 1–17) and in the coatings (points No. 18–21)

	ΣOx.[b]	SiO_2	Al_2O_3	Fe_2O_3	TiO_2	MnO	MgO	CaO	Na_2O	K_2O	P_2O_5	SO_3	Si/Al[d]
No.[a]	/g 100 g^{-1}	/g 100 g^{-1}[c]											
1	69.9	56.83	32.02	6.70	1.46	0.00	0.63	0.47	0.80	1.08	0.00	0.01	1.51
2	75.5	55.94	32.13	7.19	1.45	0.20	0.62	0.41	0.85	1.12	0.11	0.00	1.48
3	79.5	53.76	32.95	8.01	1.41	0.11	0.75	0.55	0.70	1.45	0.11	0.21	1.38
4	83.2	53.31	33.69	7.63	1.60	0.00	1.06	0.42	0.54	1.66	0.10	ND	1.34
5	86.1	55.04	32.94	6.80	0.91	0.00	0.82	0.35	0.54	2.41	0.00	0.18	1.42
6	69.3	53.81	33.06	8.36	1.06	0.00	0.92	0.66	0.34	1.70	0.09	ND	1.38
7	73.2	55.85	31.20	8.92	0.60	0.18	0.69	0.50	0.68	1.30	0.00	0.09	1.52
8	71.6	53.55	33.15	7.85	2.05	0.00	0.65	0.51	0.87	1.16	0.01	0.18	1.37
9	76.1	51.67	33.09	8.38	3.53	0.00	0.77	0.47	0.72	0.96	0.29	0.12	1.32
10	71.0	52.45	31.85	9.61	1.98	0.14	0.88	0.82	0.91	1.37	0.00	ND	1.40
11	80.6	53.14	34.63	7.12	1.76	0.00	0.69	0.39	0.59	1.06	0.53	0.09	1.30
12	85.3	55.28	30.63	8.11	1.38	0.00	0.64	0.35	0.90	2.67	0.03	0.00	1.53
13	85.7	56.03	32.02	7.62	1.23	0.00	0.63	0.45	0.58	1.20	0.21	0.03	1.48
14	81.9	53.23	33.99	7.87	1.60	0.05	0.68	0.57	0.68	1.30	0.00	0.04	1.33
15	84.9	53.41	32.11	7.47	1.59	0.19	0.78	0.53	0.62	1.56	0.32	1.43	1.41
16	78.8	54.55	32.99	7.65	1.74	0.00	0.69	0.40	0.47	1.22	0.29	0.00	1.40
17	77.1	55.58	31.76	7.38	2.14	0.01	0.75	0.51	0.59	1.29	0.00	0.00	1.48
18	67.7	53.62	28.56	11.52	1.12	0.00	1.34	0.39	0.73	2.28	0.00	0.44	1.59
19	71.6	56.62	31.30	7.42	1.23	0.01	0.82	0.54	0.50	1.32	0.24	ND	1.53
20	80.0	54.10	31.90	8.90	2.02	0.10	0.66	0.38	0.47	1.36	0.00	0.11	1.44
21	70.2	54.08	30.24	10.14	1.55	0.07	1.09	0.58	0.58	1.62	0.00	0.06	1.52
m	77.1	54.37	32.20	8.13	1.59	0.05	0.79	0.49	0.65	1.48	0.11	0.18	1.44
SD	6.1	1.40	1.37	1.17	0.59	0.07	0.18	0.11	0.15	0.46	0.15	0.34	0.08

[a]Point located in Fig. 3d (m, mean value; SD, standard deviation). [b]Sum of oxides (mass %) measured by EPMA. [c]Oxide (mass %); calculated on the basis that the sum of the oxides' mass equals 100. [d]Si/Al atomic ratio.

were $\leqslant 1\%$. The clay particles forming the wall-shaped bridge and the coatings had similar chemical compositions even if the Si/Al ratio appeared greater in the coatings (mean = 1.52) than in the wall-shaped bridge (mean = 1.42). No variation in chemical composition appeared from the centre of the bridge to the coarse grains, nor was there any from the centre of the bridge to its boundary with the voids (Fig. 3d; Table 1).

At site II the thickness of the bridge ranged from 10 to 30 μm, and it linked two coated skeleton grains of quartz, 30 μm apart (Fig. 3b, e). The bridge included fine quartz grains (0.5–2 μm in size). The backscattered electron scanning images showed that the fine material was greyish within the bridge and formed a whitish discontinuous border (0.5-μm thick) along its boundary with the voids (Fig. 3b). The fine material both within the bridge (toward the centre) and along the boundary (Fig. 3; Table 2) was analysed. The results showed that the SiO_2 content ranged from 53 to 60% for the centre of the bridge and from 54 to 63% for its border. The Al_2O_3 content ranged from 30 to 35% for the centre and from 26 to 32% for the border. The variation in the Si/Al ratio was 1.3–1.7 (mean = 1.47, standard deviation = 0.12) and 1.5–2.0 (mean = 1.64, standard deviation = 0.21) for the centre and the border, respectively. The Fe_2O_3 content ranged from 3 to 8%, TiO_2 and K_2O contents from 1 to 2% (except for one point where $K_2O = 5\%$). The MgO, Na_2O, CaO contents were less than 1%. No variation in chemical composition appeared between the wall-shaped bridge and the coatings (Fig. 3e, Table 2).

Site III was a bridge 40 μm long and 0.5–1.5 μm thick without any fine grains. It was between two coated skeleton particles of quartz (Fig. 3c, f). Because of the thinness of this bridge, each analysed volume included impregnated polyester resin. Thus, the chemical determinations were characterized by a small sum of oxides, ranging from 23 to 66% (Table 3). Nevertheless, each oxide content varied independently of the sum of oxides and therefore the determinations were considered valid and discussed. Results indicated that the SiO_2 content increased from 59.3 to 82.8% toward the centre of the bridge, whereas the Al_2O_3 content decreased from 37.3 to 13.1% (Fig. 3f, Table 3). Consequently, the Si/Al ratio varied from 1.4 to 5.3 (mean = 2.75, standard deviation = 1.52). Results obtained on sites IV to VI for similar bridges gave a sum of oxide contents $\geqslant 60\%$ (Table 4). These results showed that the SiO_2 content ranged from 53.3 to 85.5%, the

Table 2 Chemical compositions (EPMA data) for the site II (Fig. 3b and e). The analysed points were located on the borders of the wall-shaped bridge (points No. 1–10), within the bridge (points No. 11–21) and in a skeleton grain coating (points No. 22 and 23)

	ΣOx.[b]	SiO_2	Al_2O_3	Fe_2O_3	TiO_2	MnO	MgO	CaO	Na_2O	K_2O	P_2O_5	SO_3	Si/Al[d]
No.[a]	/g 100 g^{-1}	/g 100 g^{-1}[c]											
1	79.6	53.95	31.39	8.56	1.41	0.15	1.26	0.35	0.70	2.24	0.00	ND	1.46
2	74.4	63.22	26.72	5.00	0.62	0.04	0.55	0.52	1.12	1.61	0.43	0.17	2.01
3	83.3	55.91	31.95	7.61	0.92	0.10	0.94	0.40	0.68	1.44	0.06	ND	1.48
4	77.0	56.77	29.09	7.26	3.22	0.01	0.92	0.55	0.72	1.32	0.14	ND	1.66
5	67.3	63.35	26.08	4.70	1.91	0.00	0.65	0.67	1.20	1.01	0.00	0.43	2.06
6	80.0	55.92	31.52	7.09	1.94	0.00	0.84	0.41	0.73	1.38	0.16	ND	1.51
7	64.1	56.96	30.21	6.39	2.19	0.00	0.51	0.64	1.23	1.12	0.34	0.42	1.60
8	61.7	59.73	29.06	4.31	0.84	0.00	0.76	2.71	1.40	1.05	0.00	0.15	1.74
9	73.4	56.74	30.90	7.42	1.35	0.05	0.65	0.58	0.68	1.53	0.09	ND	1.56
10	71.1	56.10	31.88	6.26	1.26	0.07	0.75	0.68	0.89	1.51	0.04	0.55	1.49
11	76.7	55.69	31.75	7.03	1.50	0.00	0.84	0.44	0.72	1.59	0.43	ND	1.49
12	81.3	59.89	30.01	5.60	1.14	0.05	0.46	0.35	0.72	1.71	0.06	ND	1.69
13	78.2	55.86	33.65	5.82	1.13	0.04	0.81	0.46	0.85	1.39	0.00	0.00	1.41
14	75.8	57.99	29.96	8.00	0.63	0.21	0.60	0.55	0.68	1.22	0.00	0.16	1.64
15	82.2	53.97	32.84	7.34	1.82	0.00	0.82	0.48	0.98	1.61	0.13	ND	1.39
16	80.7	57.91	30.33	6.78	1.73	0.00	0.63	0.47	0.80	1.35	0.00	ND	1.62
17	80.1	53.72	32.77	6.07	3.43	0.00	0.82	0.38	1.24	1.53	0.02	0.02	1.39
18	83.7	55.22	32.52	6.24	1.06	0.00	0.67	0.38	1.37	1.66	0.78	0.11	1.44
19	82.4	53.24	33.18	7.56	1.82	0.16	0.76	0.42	0.75	1.46	0.49	0.16	1.36
20	75.6	54.47	32.87	6.41	1.93	0.00	1.22	0.64	0.75	1.52	0.00	0.18	1.41
21	90.1	54.57	34.88	2.94	0.49	0.14	0.61	0.28	0.66	5.12	0.13	0.18	1.33
22	81.7	56.16	31.31	6.36	2.99	0.06	0.68	0.34	0.66	1.31	0.13	ND	1.52
23	61.0	57.33	32.27	5.87	0.86	0.00	0.65	0.70	0.68	0.99	0.10	0.54	1.51
m	76.6	56.72	31.18	6.38	1.57	0.05	0.76	0.58	0.88	1.59	0.15	0.24	1.56
SD	7.4	2.71	2.09	1.29	0.81	0.06	0.20	0.48	0.25	0.82	0.20	0.18	0.19

[a]Point located in Fig. 3e (m, mean value; SD, standard deviation). [b]Sum of oxides (mass %) measured by EPMA. [c]Oxide (mass %) calculated on the basis that the sum of the oxides' mass equals 100. [d]Si/Al atomic ratio.

Table 3 Chemical composition (EPMA data) of the wall-shaped bridge in the site III (Fig. 3c and f)

	ΣOx.[b]	SiO_2	Al_2O_3	Fe_2O_3	TiO_2	MnO	MgO	CaO	Na_2O	K_2O	P_2O_5	SO_3	Si/Al[d]
No.[a]	/g 100 g^{-1}	/g 100 g^{-1}[c]											
1	25.9	82.81	13.31	0.60	1.00	0.00	0.23	0.12	0.12	0.89	0.93	0.00	5.28
2	35.5	74.55	16.70	4.20	0.78	0.06	0.36	0.42	0.28	1.37	0.84	0.42	3.79
3	22.8	67.49	21.67	6.21	1.31	0.17	0.48	0.39	0.66	1.22	0.00	0.39	2.64
4	46.2	62.22	31.38	2.40	1.75	0.13	0.73	0.39	0.15	0.67	0.17	0.00	1.68
5	65.7	61.04	29.70	4.93	1.61	0.08	0.79	0.36	0.32	0.76	0.17	0.26	1.74
6	38.4	59.29	37.34	0.40	1.59	0.00	0.81	0.00	0.03	0.16	0.18	0.21	1.35
m	39.1	67.90	25.02	3.13	1.34	0.07	0.57	0.28	0.26	0.84	0.38	0.21	2.75
SD	15.6	9.17	9.29	2.38	0.38	0.07	0.24	0.18	0.22	0.43	0.40	0.18	1.52

[a]Point located in Fig. 3f (m, mean value; SD, standard deviation). [b]Sum of oxides (mass %) measured by EPMA; [c]Oxide (mass %) calculated on the basis that the sum of oxides' mass equals 100. [d]Si/Al atomic ratio.

Al_2O_3 content from 9.5 to 34.0% and the Fe_2O_3 content from 2.8 to 9.3%. The contents of K_2O, TiO_2, MgO, Na_2O and CaO components were similar to those measured on thicker bridges (Tables 1 and 2).

Discussion

The XRD analysis of the <0.5 μm fraction showed the presence of kaolinite, quartz and both expanding (smectite)

Table 4 Chemical composition (EPMA data) of several longest wall-shaped bridges (sites IV to VI)

	ΣOx.[b]	SiO_2	Al_2O_3	Fe_2O_3	TiO_2	MnO	MgO	CaO	Na_2O	K_2O	P_2O_5	SO_3	Si/Al[d]
No.[a]	/g 100 g^{-1}	/g 100 g^{-1}[c]											
1	75.8	85.53	9.52	2.81	0.39	0.00	0.33	0.13	0.29	0.39	0.24	0.37	7.63
2	79.5	55.00	31.22	9.27	1.18	0.00	0.77	0.29	0.67	1.48	0.00	0.11	1.50
3	89.5	64.01	24.44	5.73	1.39	0.00	0.60	0.36	0.57	2.17	0.74	0.00	2.22
4	63.2	53.31	33.99	7.46	1.49	0.00	0.85	0.44	0.69	1.65	0.03	0.09	1.33
5	85.9	58.79	29.84	6.04	1.17	0.01	0.66	0.28	0.86	2.33	0.00	0.03	1.67
6	64.6	57.01	31.08	6.66	1.14	0.00	0.65	0.57	0.45	2.03	0.00	0.42	1.56
7	89.9	63.30	22.90	4.67	0.42	0.02	0.31	0.13	0.56	7.56	0.00	0.12	2.35
8	68.8	62.79	26.98	5.79	1.60	0.00	0.53	0.42	0.32	1.17	0.00	0.39	1.97
9	81.7	63.87	26.43	5.36	1.46	0.05	0.54	0.28	0.29	1.66	0.07	0.00	2.05
10	83.1	67.90	22.49	4.55	1.08	0.00	0.61	0.34	0.44	2.06	0.53	0.00	2.56
11	66.8	62.21	28.13	5.80	1.04	0.00	0.61	0.31	0.24	1.23	0.27	0.15	1.88
12	80.4	56.02	31.99	7.83	1.10	0.16	0.74	0.43	0.43	1.10	0.11	0.10	1.49
13	75.1	58.10	31.00	6.06	1.36	0.00	0.67	0.40	0.49	1.75	0.09	0.08	1.59
14	73.3	66.85	21.64	5.93	2.69	0.00	0.60	0.28	0.37	1.22	0.37	0.05	2.62
15	80.2	57.17	31.06	6.24	0.87	0.00	0.82	0.51	0.25	2.83	0.10	0.16	1.56
m	77.2	62.12	26.85	6.01	1.23	0.02	0.62	0.34	0.46	2.04	0.17	0.14	2.26
SD	8.6	7.82	6.14	1.49	0.53	0.04	0.15	0.12	0.18	1.64	0.22	0.14	1.54

[a]Point from the undifferentiated sites IV, V and VI (m, mean; SD, standard deviation). [b]Sum of oxides (mass %) measured by EPMA. [c]Oxide (mass %) calculated on the basis that the sum of oxides' mass equals 100. [d]Si/Al atomic ratio.

and nonexpanding (illite) 2 : 1 clay in the loose and hard horizons. On the diffractograms of the hard horizon (Fig. 2b, c) the peak at 0.154 nm can be related to d (211) quartz or d (060) trioctahedral 2 : 1 clay minerals (Brindley & Brown, 1980). Although the 2 : 1 clay content increased with depth, the intensity of the peak at 0.154 nm decreased, indicating a decrease in the quartz content. Thus, the 2 : 1 clay would be dioctahedral as indicated by the 0.149 nm peak. This peak, which is asymmetric towards smaller angles could represent the sum of the contributions of kaolinite, illite and 2 : 1 clay minerals. The relative amounts of the minerals varied in the profile. The proportion of expanding 2 : 1 clay minerals increased with depth, particularly in the hard horizon. Similar XRD results were obtained on the clay fraction of Solonetz in Chad by Paquet (1970) and of Planosols in Nigeria by Esu (1989). Furthermore, the increase in smectite proportion with depth is consistent with the results obtained for Solonetz and Planosol in Chad (Bocquier *et al.*, 1970; Paquet, 1970) or Burkina Faso (Boulet & Paquet, 1972) and for Montana Solonetz (Klages & Southard, 1968).

All of the chemical results show the composition of wall-shaped bridges and coatings to be homogeneous (Tables 1–4): SiO_2, Al_2O_3 and Fe_2O_3 were the major components, and K_2O, TiO_2, MgO, Na_2O and CaO are associated with them. No significant variation in P_2O_5 and SO_3 contents appeared, thus indicating there was no variation in the components which included P and S, particularly the organic matter (McKeague & Protz, 1980).

The data reported in the Si, Al, K + Ca + Na and Si, Al, Fe triangular diagrams show little variation between the sites analysed (Fig. 4a, b, c). The compositions of reference minerals were also plotted within these diagrams. These minerals were selected on the basis of the XRD results on the extracted <0.5 μm fraction, which showed the presence of kaolinite, quartz and 2 : 1 clay minerals. Illite and smectite were selected as reference minerals for 2 : 1 clay minerals with nonswelling and swelling d-spacing, respectively. The triangular diagrams indicate that the results of chemical analysis are intermediate between the reference minerals (Fig. 4). Considering the size of the volume analysed (3–5 μm^3) and the very small size of the particles that form the wall-shaped bridges, the results indicate that mixtures of minerals were analysed. These mixtures are composed mainly of Al-Fe beidellite (Paquet, 1970; Tardy, 1981; Duplay, 1982), and secondarily of kaolinite, illite and quartz. The presence of Al-Fe beidellite is consistent with the dioctahedral nature of the smectite as deduced from the XRD diffractograms (Fig. 2b, c).

The main variation in chemical composition concerned the Si/Al ratio (Tables 1–4). It revealed differences in the mineralogical composition between the analysed volumes. For a Si/Al ratio of from 1.3 to 2, the wall-shaped bridges consisted mostly of Al-Fe beidellite with very small contents of kaolinite, illite and silica (quartz or amorphous silica). The increase in silica was associated with a decrease in the Fe/Si ratio. Therefore, it was not associated with an increase in Fe-rich smectite (nontronite) content, thus confirming the presence of Al-Fe

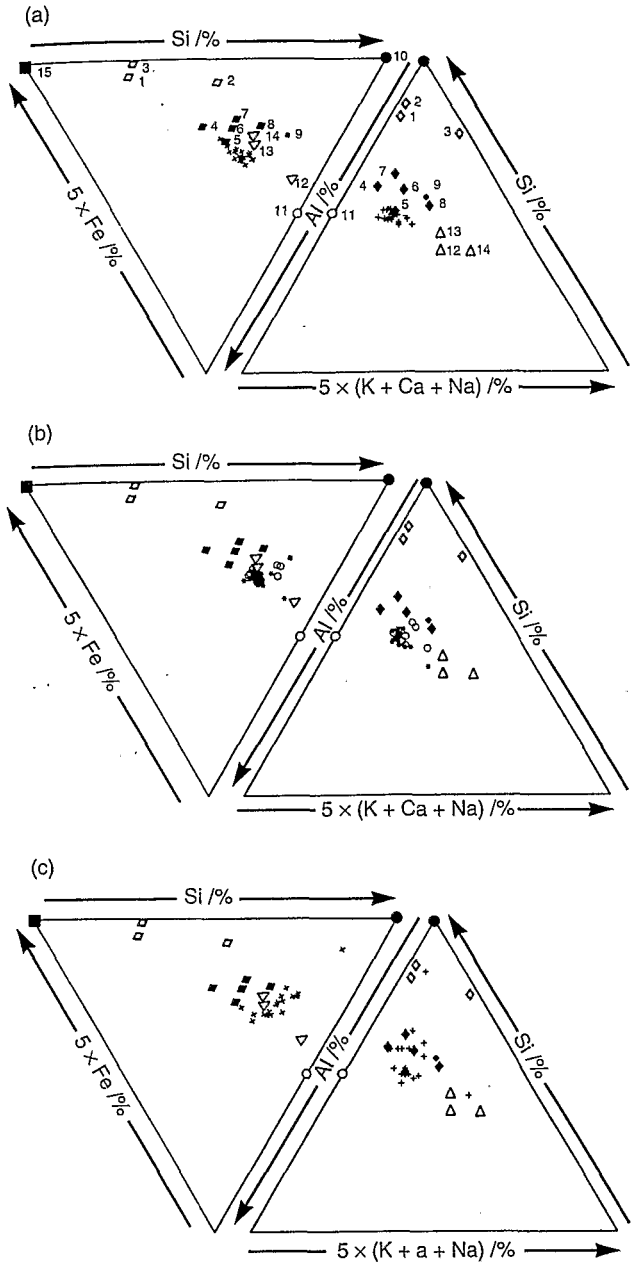

Fig. 4 Si, Al, 5 × Fe and Si, Al, 5 × (K + Ca + Na) composition (expressed as atomic element) of wall-shaped bridges and coatings (a) at site I (+, EPMA data), (b) at site II (○, and *, EPMA data obtained on the border and within the bridge, respectively), (c) at site III (+, EPMA data). Composition of reference minerals: ◇, 1, Pennsylvania Nontronite (Duplay, 1982); ◇, 2, Nontronite (Weaver & Pollard, 1973); ◇, 3, Chad Nontronite (Tardy, 1981); ◆, 4, Godola Fe-Al Beidellite (Duplay, 1982, 1989); ◆, 5, Fe-Al Beidellite (Duplay, 1982); ◆ 6, Kfar-Zabad Fe-Al Beidellite (Paquet, 1970); ◆, 7, Chad Fe-Al Beidellite (Tardy, 1981); ◆, 8, Upton-Wyoming Fe-Al Beidellite (Newman & Brown, 1987); •, 9, Aberdeen Montmorillonite (Newman & Brown, 1987); ●, 10, quartz; ●, 11, theoretic kaolinite; △, 12, Bothamsall Illite (Warren & Curtis, 1989); △, 13, Fithian Illite (Robert & Barshad, 1972); ○, △, 14, Puy Illite (Robert & Barshad, 1972); ■, 15, Fe-oxide.

beidellite. Because there was no evidence of amorphous or poorly ordered silica, the increase in the Si/Al ratio for Si/Al $\geqslant 2$ especially, can be attributed to an increase in the quartz content in a mixture dominated by Al-Fe beidellite. Indeed, the wall-shaped bridges included quartz grains (0.5–3 μm in size) as shown in Fig. 3.

The wall-shaped bridge analysed at site I (Fig. 3a, d) showed no evidence of well-ordered variations in chemical composition across or along the bridge (Table 1; Fig. 4a). At site II (Fig. 3b, e) the fine material on the border consisted mostly of silica and was more heterogeneous than toward the centre of the bridge (Table 2; Fig. 4b). The variation in the Si/Al ratio cannot explain the difference in brightness between the centre and the boundary of the bridge (Lloyd, 1987). Hence, the difference in brightness would be related to the border effects, thus enabling a higher emission of back-scattered electrons on the boundary of the bridge. The results from the other sites (Tables 3 and 4) confirmed that the longest bridges have the greatest SiO_2 contents, the smallest Al_2O_3 contents, and therefore (Table 4) the greatest Si/Al ratios (mean = 2.26) with the maximum of variation (standard deviation = 1.54). Most of the chemical compositions of these longest bridges plotted within triangular diagrams (Fig. 4c) are comparable with the composition of several Fe-Al beidellites even if their distribution was greater and they had large Si contents.

The mineralogical interpretation of the chemical analysis indicated that the coating and bridging fine material consist mainly of Al-Fe beidellite with small amounts of kaolinite, illite, quartz and possible amorphous silica (Fig. 5). It appeared also that the silica content varies weakly with the morphology of bridges. These results strongly differed from the XRD results obtained on the $\leqslant 0.5$ μm fraction where kaolinite prevails associated with smaller amounts of smectite, illite and quartz. Indeed, the dispersion of the bulk samples by shaking would produce kaolinite particles from the weathered feldspar grains and would explain the concentration of kaolinite in the extracted fraction.

On the other hand, the mineralogy deduced from EPMA is consistent with the soil mineralogy encountered under arid pedoclimates (Borchardt, 1989; Eghbal & Southard, 1993). Kaolinite could be relict from the parent material or from feldspar weathering under a wetter climate. In addition, an aeolian deposition of kaolinite cannot be also eliminated, as suggested by Eghbal & Southard (1993).

The wall-shaped bridges have meniscus shapes (Lamotte *et al.*, 1997). Their formation could result from the evaporation of the soil solution under arid conditions, thus inducing the concentration of inherited Fe-Al beidellite or its neoformation during the concentration of the soil solution at the top of the hard horizon (Lamotte *et al.*, 1997). Other inherited mineral species, initially in suspension in the soil solution, such as kaolinite, illite and quartz would have been included within the clay matrix. Finally, the wall-shaped bridges which formed the

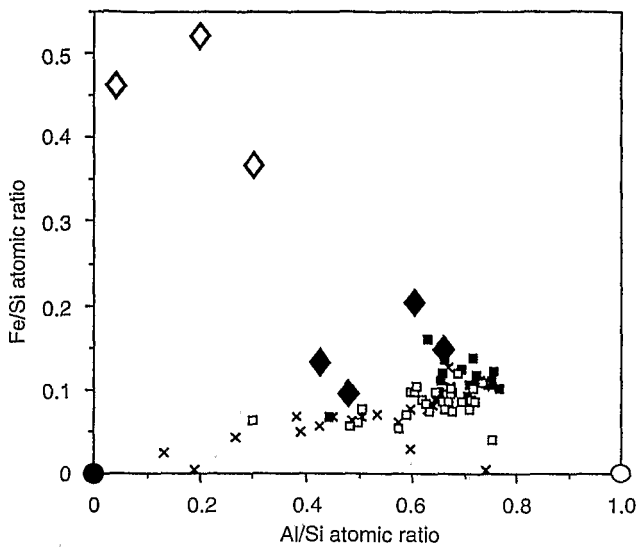

Fig. 5 Related variation of Fe/Si and Al/Si atomic ratios for the whole results of the wall-shaped bridges and the coatings which were analysed from site I (■, EPMA data), site II (□, EPMA data) and sites III to VI (×, EPMA data) and the composition of reference minerals (◇, nontronite; ◆, Al-Fe beidellite; ○, kaolinite; ●, quartz).

continuity between the coated skeleton grains are composed mainly of smectite. Larger concentrations of silica along the longest and finest wall-shaped bridges could indicate a small excess of silica in the solution during neoformation, but this cannot be responsible for the soil hardness. In the dry state, the close packing of the clay particles, face to face, with intense particle interactions provides continuity of the solid phase and very strong cohesion (Tessier & Pédro, 1984). On wetting the clay particles swell, the interparticle clay cohesion decreases and finally the soil disperses in water, thus explaining the difference in hardness between the dry and wet states.

Conclusion

The bonding agent constituting both the coatings and the wall-shaped bridges in the hard horizon consists of prevailing Al-Fe beidellite with varying small amounts of kaolinite, illite and quartz and possible amorphous silica. Even if the chemical composition and particularly the silica content varies somewhat with the morphology of the wall-shaped bridges, the chemical composition was fairly homogeneous. Successive layers were not differentiated according to their chemical composition.

The geochemistry of the bonding agent is consistent with the mineralogy of clays currently encountered in arid climates. The development of both the coatings and the wall-shaped bridges which have a meniscus shape could result from an evaporation process which induced (i) either the concentration of inherited Al-Fe beidellite, kaolinite, illite and quartz initially present in the sedimentary material, or (ii) the neoformation of Al-Fe beidellite, the latter smectite being mixed with inherited fine particles (kaolinite, illite and quartz) initially present in the soil solution. Consequently, the mixture forms a deposit on the skeleton grains (coatings) and in the intergranular voids (wall-shaped bridges).

The morphological and mineralogical studies of the fabric showed that a small amount of clay particles is required to generate a continuity of the solid phase from the coatings on the grains to the intergranular wall-shaped bridges. The clayey bonding agent is responsible for the fabric's hardness because the clay particles are very small and so can bind elementary particles at short distances. Finally, without any cementing agent, the characteristics of the fabric and the composition of the bonding agent explain the hardness in the dry state and may possibly explain the slaking in water.

Acknowledgements

We thank M. Hardy (Institut National de la Recherche Agronomique, Orléans) and G. Millot (Institut Français de Recherche Scientifique pour le Développement en Coopération, Bondy) for XRD measurements, C. Gilles (Bureau de Recherches Géologiques et Minières, Orléans), O. Rouer and B. Guillet (Centre National de la Recherche Scientifique, Orléans) for their help and device in EPMA.

References

Balbir-Singh & Gilkes, R.J. 1993. The recognition of amorphous silica in indurated soil profiles. *Clay Minerals*. **28,** 461–474.

Bocquier, G., Paquet, H. & Millot, G. 1970. Un nouveau type d'accumulation oblique dans les paysages géochimiques: l'invasion remontante de la montmorillonite. *Comptes Rendus de l'Académie des Sciences de Paris. Série D*, **271,** 460–463.

Borchardt, G. 1989. Smectites. In: *Minerals in Soil Environments*, Second edn (eds J.B. Dixon and S.B. Weed), pp. 675–727. Soil Science Society of America, Madison, WI.

Boulet, R. & Paquet, H. 1972. Deux voies différentes de la pédogenèse en Haute-Volta. Convergence finale vers la montmorillonite. *Comptes Rendus de l'Académie des Sciences de Paris. Série D*, **275,** 1203–1206.

Bridges, E.M. & Bull, P.A. 1983. The role of silica in the formation of compact and indurated horizons in the soils of South Wales. In: *Soil Micromorphology, Proceedings of the 6th International Working Meeting on Soil Micromorphology, London* (eds P. Bullock and C.P. Murphy), pp. 605–613. A. B. Academic Publishers, Berkhamsted, UK.

Brindley, G.W. & Brown, G. 1980. *Crystal Structures of Clay Minerals and their X-ray Identification* (Reprinted 1984) (eds G.W. Brindley and G. Brown), Mineralogical Society Monograph, Mineralogical Society, London.

Chartres, C.J. & Fitzgerald, J.D. 1990. Properties of siliceous cements in some Australian soils and saprolites. *Developments in Soil Science*, **19,** 199–206.

Duplay, J. 1982. *Populations de particules d'argiles. Analyse chimique par microsonde électronique*. Thèse de 3ème Cycle, Université de Poitiers.

Duplay, J. 1989. *Géochimie des argiles et géothermométrie des populations monominérales de particules*. Thèse d'Etat, Université de Strasbourg.

Eghbal, M.K. & Southard, R.J. 1993. Mineralogy of Aridisols on dissected alluvial fans, western Mojave Desert, California. *Soil Science Society of America Journal*, **57,** 538–544.

Esu, I.E. 1989. A pedological characterization of soils of the Hadejia alluvial complex in the semi-arid region of Nigeria. *Pédologie*, **34,** 171–190.

FAO–UNESCO. 1975. *Soil Map of the World (1/5 000 000)*. FAO, Paris.

Franzmeier, D.P., Norton, L.D. & Steinhardt, G.C. 1989. Fragipan formation in loess of the midwestern United States. In: *Fragipans: Their Occurrence, Classification and Genesis* (eds N.E. Smeck and E.J. Ciolkosz), pp. 69–97. Soil Science Society of America, Special Publication No 24, Madison, WI.

Grossman, R.B., Fehrenbacher, J.B., Beavers, A.H., Stephen, I. & Parker, J.M. 1959. Fragipan soils of Illinois, I, II and III. *Soil Science Society of America Proceedings*, **23,** 65–75.

Harlan, P.W., Franzmeier, D.P. & Roth, C.B. 1977. Soil formation on loess in southwestern Indiana: II. Distribution of clay and free oxides and fragipan formation. *Soil Science Society of America Journal*, **41,** 99–103.

Jha, P.P. & Cline, M.G. 1963. Morphology and genesis of a sol brun acide with fragipan in uniform silty material. *Soil Science Society of America Proceedings*, **27,** 339–344.

Klages, M.G. & Southard, A.R. 1968. Weathering of montmorillonite during formation of a solodic soil and associated soils. *Soil Science*, **106,** 363–368.

Lamotte, M. 1995. *Les sols à forte cohésion des zones tropicales arides. Étude du hardé Lagadgé au Nord-Cameroun*. Collection TDM, ORSTOM, Paris.

Lamotte, M., Bruand, A., Humbel, F.X., Herbillon, A. & Rieu, M. 1997. A hard sandy-loam soil from semi-arid Northern Cameroon: I. Fabric of the groundmass. *European Journal of Soil Science*, **48,** 213–225.

Lindbo, D.L. & Veneman, P.L.M. 1989. Fragipans in the northeastern United States. In: *Fragipans: Their Occurrence, Classification and Genesis* (eds N.E. Smeck and E.J. Ciolkosz), pp. 11–31. Soil Science Society of America, Special Publication No 24, Madison, WI.

Lloyd, G.E. 1987. Atomic number and crystallographic contrast images with the SEM: a review of backscattered electron techniques. *Mineralogical Magazine*, **51,** 3–19.

Lozet, J.M. & Herbillon, A.J. 1971. Fragipan soils of Condroz (Belgium). Mineralogical, chemical and physical aspects in relation with their genesis. *Geoderma*, **5,** 325–343.

McDonald, R.C., Isbell, R.F., Speight, J.G., Walker, J. & Hopkins, M.S. 1984. *Australian Soil and Land Survey, Field Handbook*. Inkata Press, Melbourne.

McKeague, J.A. & Protz, R. 1980. Cement of duric horizons, micromorphology and energy dispersive analysis. *Canadian Journal of Soil Science*, **60,** 45–52.

Milnes, A.R., Wright, M.J. & Thiry, M. 1991. Silica accumulations in saprolites and soils in south Australia. In: *Occurrence, Characteristics and Genesis of Carbonate, Gypsum and Silica Accumulations in Soils* (ed. W.D. Nettleton), pp. 121–149. Soil Science Society of America, Special Publication No 26, Madison, WI.

Mullins, C.E. & Ley, G.J. 1995. Mechanisms and characterisation of hardsetting in soils. In: *Sealing, Crusting, Hardsetting Soils: Productivity and Conservation* (eds H.B. So, G.D. Smith, S.R. Raine, B.M. Schafer & R.J. Loch), pp. 157–170. ASSSI, Brisbane.

Newman, A.C.D. & Brown, G. 1987. The chemical constitution of clays. In: *Chemistry of Clays and Clay Minerals* (ed. A.C.D. Newman), pp. 1–128. Mineralogical Society Monograph No 6, Longman, Harlow, UK.

Norton, L.D., Hall, G.F., Smeck, N.E. & Bigham, J.M. 1984. Fragipan bonding in a Late-Wisconsinan loess-derived soil in east-central Ohio. *Soil Science Society of America Journal*, **48,** 1360–1366.

Paquet, H. 1970. *Evolution géochimique des minéraux argileux dans les altérations et les sols des climats méditerranéens tropicaux à saisons contrastées*. Thèse d'Etat, Université de Strasbourg.

Pouchou, J.L. 1987. Pratique de la spectrométrie WDS. In: *Microanalyse par sonde électronique: spectrométrie de rayons X* (eds D. Benoit, F. Grillon, F. Maurice, N. Roinel, J. Ruste and R. Tixier), pp. E1–E23. Association Nationale de la Recherche et de la Technologie, Paris.

Robert, M. & Barshad, I. 1972. Sur les propriétés et la détermination des minéraux 2/1 expansibles (vermiculites-smectites). *Comptes Rendus de l'Académie des Sciences de Paris*. Série D, **275,** 1463–1465.

Smeck, N.E. & Ciolkosz, E.J. (eds) 1989. *Fragipans: Their Occurrence, Classification and Genesis*, Soil Science Society of America, Special Publication No 24, Madison, WI.

Soil Survey Staff. 1975. *Soil Taxonomy. A Basic System of Soil Classification for Making and Interpreting Soil Surveys*. US Government Printing Office, Washington, DC.

Tardy, Y. 1981. Silice, silicates magnésiens, silicates sodiques et géochimie des paysages arides. *Bulletin de la Société Géologique de France*, **23,** 325–334.

Tessier, D. & Pédro, G. 1984. Recherches sur le rôle des minéraux argileux dans l'organisation et le comportement des sols. In: *Livre jubilaire du cinquantenaire AFES.*, pp. 223–234. Association Française pour l'Etude du Sol, Paris.

Wang, C., Nowland, J.L. & Kodama, H. 1974. Properties of two fragipan soils in Nova Scotia including scanning electron micrographs. *Canadian Journal of Soil Science*, **54,** 159–170.

Warren, E.A. & Curtis, C.D. 1989. The chemical composition of authigenic illite within two sandstone reservoirs as analysed by ATEM. *Clay Minerals*, **24,** 137–156.

Weaver, C.E. & Pollard, L.D. 1973. *The Chemistry of Clay Minerals*. Elsevier, Amsterdam.

Yassoglou, N.J. & Whiteside, E.P. 1960. Morphology and genesis of some soils containing fragipans in northern Michigan. *Soil Science Society of America Proceedings*, **24,** 396–407.